Precision Engineering 74 (2022) 242–246

Contents lists available at ScienceDirect

Precision Engineering

journal homepage: www.elsevier.com/locate/precision

Concentric ring structure on the front surface of fused silica induced by a focused femtosecond pulse laser

Lin Zhang, Jiamin Liu, Hao Jiang *, Shiyuan Liu **

State Key Laboratory of Digital Manufacturing Equipment and Technology, Huazhong University of Science and Technology, Wuhan, 430074, China

ARTICLE INFO

Keywords:
Femtosecond laser damage
Concentric ring structure
Ablation

ABSTRACT

Structural changes of the transparent materials induced by a Femtosecond laser play an important role in the field of femtosecond laser micromachining. In this paper, a concentric ring structure with a period of 2 μm has been observed on the front surface when a single femtosecond pulse was focused at 15 μm below the fused silica surface with an input pulse energy of 2 mJ. A linear correlation between the size of the concentric ring structure and the input pulse energy has been revealed. A model based on the nonlinear Schrödinger equation has been used to calculate the radial light intensity distribution on the fused silica surface. The calculated light intensity distribution and the experimental results are well mapped to each other, which can be expected to provide a new perspective for the exploration of the formation mechanism of the laser-induced concentric ring structure.

1. Introduction

In recent years, femtosecond laser micromachining has become an emerging technology in the field of material processing by means of focusing the beam on the surface or inside of the material [1]. When the ultrafast laser is focused on the sample surface or near the surface, the laser energy will be deposited around the focal area and be absorbed by the surface material in an ultra-short time, which induces the material to be ablated. As a result, the material peels off from the surface, forming a series of regularly arranged groove structures, the so-called laser--induced periodic surface structures (LIPSS) [2–5]. For many materials, it has been demonstrated that the morphological characteristics of LIPSS, such as the period and the depth of the groove, can be well manipulated by the irradiation fluence, the temporal shaping, the polarization state, the pulse number, and the incidence angle of the laser pulse [6–10]. The reported good controllability of the structural characteristics, coupled with the simple processing steps, enable LIPSS to have a large number of technical applications, such as structural color, antibacterial surfaces, chemical analytics, etc. [2,11]. As a widely used optical element material, the structure damage of silica glass has been widely studied under the condition of ultrafast laser irradiation [12–14]. Interestingly, different from the parallel arrangement of the groove structure shown by the typical LIPSS feature, a concentric ring structure on the fused silica surface was induced by the ultrafast laser. Heins AM et.*al* studied the concentric ring structure induced by a fs laser pulse on the surface of glass, and proved that the appearance of the rings is related to the ambient medium [15,16]. At the same time, the formation of periodic annular surface structure on the fused silica surface induced by multiple fs laser pulses was reported by Liu Y et.*al* [17]. Zhang X et.*al* reported that a concentric ring structure is formed on the front surface when the laser pulse is focused on the rear surface of the fused silica [18]. The formation of the concentric ring structure on the fused silica surface adds new characteristics to the LIPSS. However, the exact relationship between these new characteristics and the input pulse energy is rarely discussed.

In order to understand the formation mechanism of the laser-induced concentric ring structure, it is important to consider the nature of the interaction between ultrafast lasers and materials. For the description of femtosecond laser irradiation in fused silica, the model based on the nonlinear Schrödinger equation and the free-electron density rate equation is widely used [19–24], which mainly describes the effects of beam diffraction, multiphoton absorption, plasma defocusing and Kerr self-focusing. In addition, some theoretical models based on interference or diffraction have also been proposed to explain the formation of the structure [17,25,26]. These controversial discussions suggest that more experimental and theoretical studies are required to further reveal the formation mechanism of the laser-induced concentric ring structure.

In this paper, a concentric ring structure with a period of 2 μm has

* Corresponding author.
** Corresponding author.
E-mail addresses: hjiang@hust.edu.cn (H. Jiang), shyliu@hust.edu.cn (S. Liu).

https://doi.org/10.1016/j.precisioneng.2021.12.004
Received 13 September 2021; Received in revised form 9 December 2021; Accepted 12 December 2021
Available online 14 December 2021

been obtained on a silica surface when a single femtosecond pulse was focused at 15 μm below the fused silica surface. A linear relationship between the size of the concentric ring structure and the input pulse energy has been demonstrated by varying the input pulse energy. Furthermore, a model based on the nonlinear Schrödinger equation was used to calculate the radial light intensity distribution. Results show that the radial intensity presents a concentric ring-shaped distribution which is consistent with the concentric ring structure observed in the experiment.

2. Experiment and theory

2.1. Experiment

In this work, a Ti: sapphire ultrafast laser system (Solstice Ace, Spectra Physics Ltd.) was used to deliver 35 fs pulses with a nominal repetition of 1 kHz. It can be adjusted in integer multiples from 1 Hz to 1 kHz and in this work the repetition was set as 10 Hz. Meanwhile, a mechanical shutter (SH1/M, THORLABS) with open time of 0.1 s was used to ensure the single pulse shot. The central wavelength is 800 nm. The maximum energy of the single pulse was 7 mJ. The diameter of the output laser beam is 16 mm. A plano-convex lens (LA1951-B, THORLABS) with focal length $f = 25.4$ mm has been used to focus the beam. The diameter of the ionized air plasma is measured to be about 80 μm when the femtosecond laser was focused in the air by this lens [27]. The focal plane is set as 15 μm below the sample front surface. It can be estimated that the spot size of the laser irradiated on the silica surface was approximate 100 μm. The size of the fused silica sample is 10 × 10 × 6 mm^3, the impurity content is 5 ppm and all the surfaces have been polished with a nominal roughness of 5 nm to ensure good transmittance and uniformity. The sample was mounted on a three-axis translation stage to ensure that each shot can be focused on a fresh position of the sample by moving the stage, as shown in Fig. 1. All the experiments were carried out in the ultra-clean room. The experimental variables, such as the incident angle of the laser, the position of the focal point, and the input pulse energy were strictly controlled to guarantee the processing quality and processing consistency. Moreover, the ablation experiments were repeated twice under the same conditions to ensure the reproducibility of the results. The detailed observation of the ablation area was performed by an optical microscope, a SEM (Quanta 200, FEI Ltd.) and an AFM (SPM9700, Shimadzu).

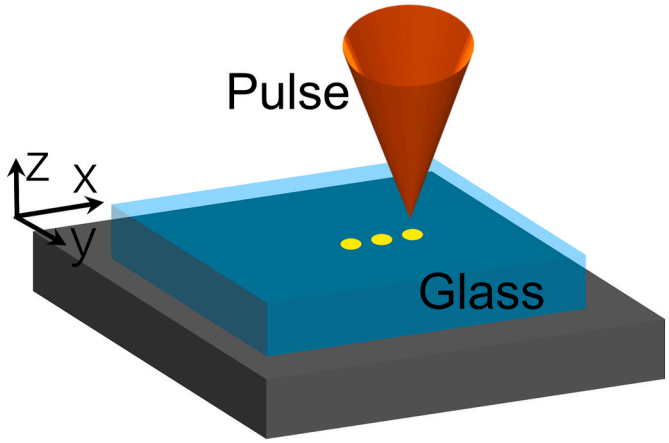

Fig. 1. The schematic diagram of sample ablation.

2.2. Theory

The propagation of the focused femtosecond laser in the transparent material is complicated, made up of a series of linear and nonlinear effects, such as beam diffraction, group velocity dispersion, multiphoton absorption, free-carrier absorption and plasma defocusing, as well as Kerr self-focusing. In this work, a model based on the nonlinear Schrödinger equation and the free-electron density rate equation was used to study the light intensity distribution. The nonlinear Schrödinger equation can be expressed as

$$\frac{\partial E}{\partial z}=\frac{i}{2k}\left(\frac{\partial^2}{\partial r^2}+\frac{1}{r}\frac{\partial}{\partial r}\right)E-\frac{ik''}{2}\frac{\partial^2 E}{\partial \xi^2}-\frac{\sigma}{2}(1+i\omega\tau_c)\rho E-\frac{1}{2}\beta^{(K)}|E|^{2K-2}E+ik_0n_2|E|^2E\,, \tag{1}$$

where z is the propagation distance, r is the radius in the calculation. k and ω_0 are the wave number and the frequency of the incident wave, respectively. n_0 is the linear refractive index and n_2 is the nonlinear refraction index, and c represents the light speed in vacuum. k'' is the coefficient of the group velocity dispersion, and ξ represents the retarded time variable. For the plasma absorption process, σ is the cross-section area for inverse bremsstrahlung. The free electron density term ρ in Eq. (1) can be described by the rate equation, which has the following expression,

$$\frac{\partial \rho}{\partial t}=\frac{1}{n_0^2}\frac{\sigma}{E_g}\rho|E|^2+\frac{\beta^{(K)}}{K\hbar\omega}|E|^{2K}-\frac{\rho}{\tau_r}, \tag{2}$$

where E_g is the gap energy, and K is the number of photons for multiphoton ionization. $\beta^{(K)}$ is the corresponding absorption coefficient. E on the left-hand side of Eq. (1) is a linearly polarized Gaussian beam with cylindrical symmetry which can be described by a complex electric field envelope, shown as

$$E(r,\xi,0)=\sqrt{\frac{2P_{in}}{\pi r_0^2}}\exp\left(-\frac{r^2}{r_0^2}-\frac{\xi^2}{\tau_0^2}-\frac{ikr^2}{2f}\right), \tag{3}$$

where r_0 is the radius of the beam on the silica surface, with a pulse duration of $\tau_0 = 35$ fs. f in the last term of Eq. (3) represents the curvature of the wave at the location with a distance d from the geometric focus. P_{in} is the input pulse power.

A split-step Fourier method has been used to solve the above-mentioned model. As a result, the spatial distribution of light intensity can be calculated.

3. Results and discussion

In order to understand the structural characteristics of the fused silica ablated by the femtosecond laser, different energies of the input pulse have been focused into the fused silica 15 μm below the surface to ablate the glass. The results and the corresponding discussion are shown below.

Fig. 2 shows the SEM image of the formed ablation area induced by a single femtosecond pulse. The input pulse energy $E_{in} = 2$ mJ, which was measured by a power meter. It can be seen that a perfect concentric ring structure was formed with a diameter of about 155 μm.

Furthermore, the influence of input pulse energy on the characteristics of the ablation area was studied. Fig. 3 shows the optical images of the ablation area with input pulse energy of 1 mJ, 2 mJ, 3 mJ, 4 mJ, 5 mJ and 5.8 mJ. The ablation experiments under the same conditions were

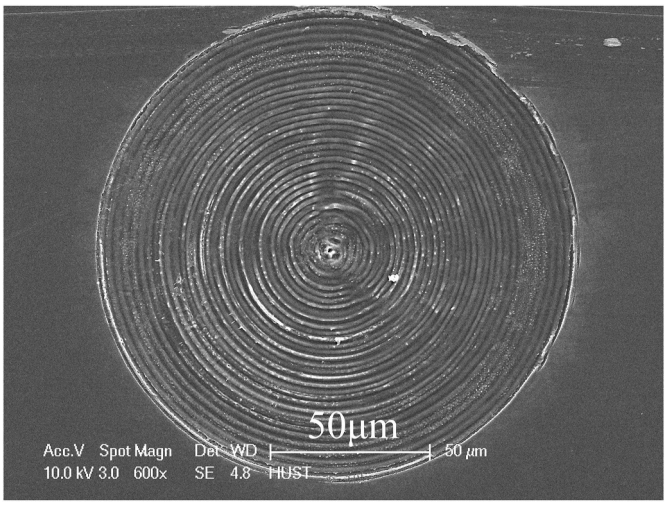

Fig. 2. SEM image of the formed concentric ring structure. The input pulse energy E_{in} = 2 mJ. The diameter of the ablation area is about 155 μm.

repeated twice to show the processing consistency. It can be seen from the results that the concentric structure can be obtained for pulses with different energy. Through further observation of the structure, it can be found that discrete point structure appears based on the ring structure. In the results of E_{in} = 5 mJ and E_{in} = 5.8 mJ, there is a circle of powdery substance around the ring structure. For this phenomenon, we give the following explanation. Due to the focusing of the femtosecond laser, the fused silica surface will accumulate extremely high temperatures in an ultrashort time, and the accumulated temperature will increase as the input pulse energy increases. In the situation of high input pulse energy, the ultrahigh temperature will melt part of the ring material after the ring structure is formed. Subsequently, the molten material will re-solidify due to the drop in temperature and will finally accumulate around the ring structure.

In addition, it can be found from Fig. 3 that the size of the ablated area is dependent on the input pulse energy. Fig. 4 shows the pulse energy dependence of the diameter of the ablation area. The black balls in the figure are the measured results and the solid line is the result of the linear fitting with R^2 = 0.975. Results show that the diameter of the ablation area changes linearly with the input pulse energy. The existence of such linear relationship indicates that under the premise of fixing other parameters, a concentric ring structure with specific size can be obtained by controlling the input pulse energy. In addition, it is conceivable that the size of the concentric ring structure is related to the spot size irradiated on the fused silica surface, which requires further study.

In order to further depict the characteristics of the concentric ring structure, an AFM was used to observe the ablation area. Fig. 5 shows the AFM image of the concentric ring structure with an area of 30 μm × 30 μm under the condition of E_{in} = 1 mJ. It can be found that the groove

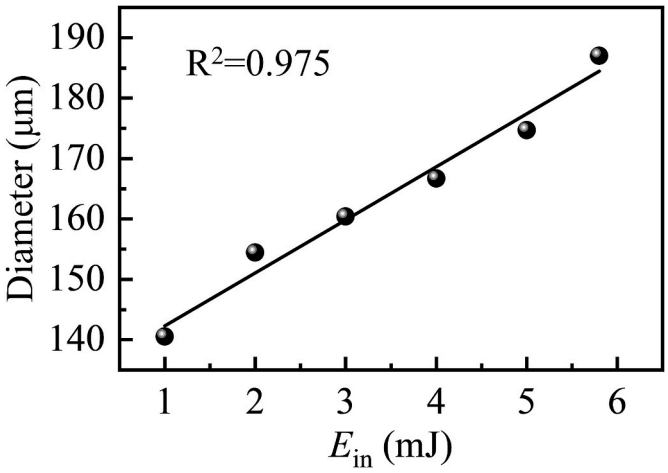

Fig. 4. The pulse energy dependence of the diameter of the ablation area. Black balls are the measured results and the solid line is the result of the linear fitting with R^2 = 0.975.

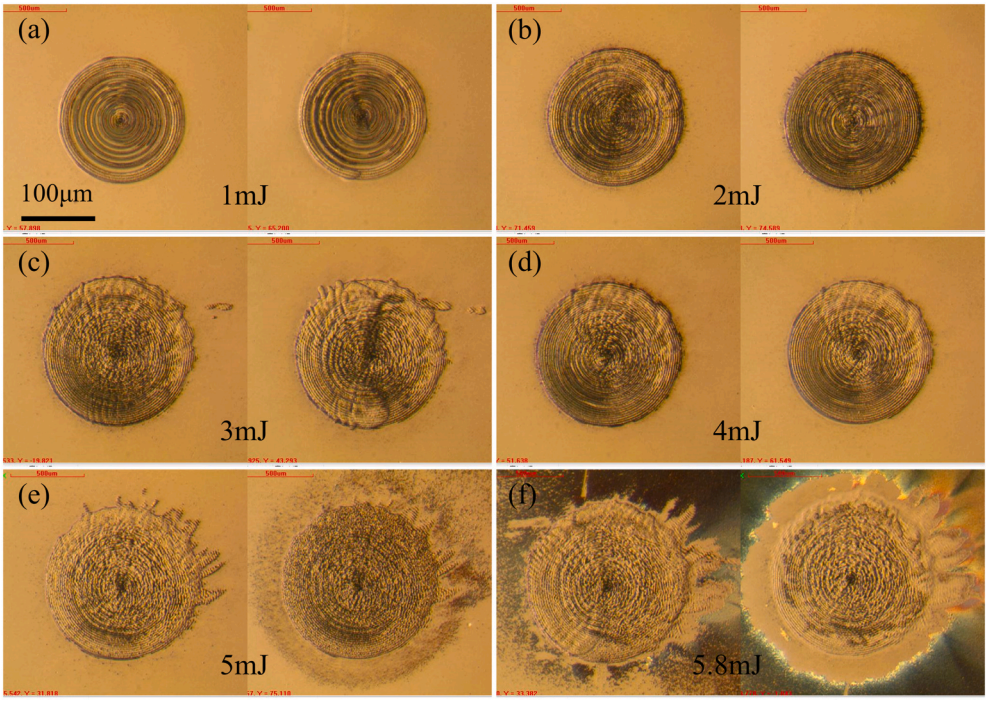

Fig. 3. The optical images of the ablation area with input pulse energy of (a) 1 mJ, (b) 2 mJ, (c) 3 mJ, (d) 4 mJ, (e) 5 mJ, (f) 5.8 mJ. The ablation experiments under the same conditions were repeated twice to show the processing consistency.

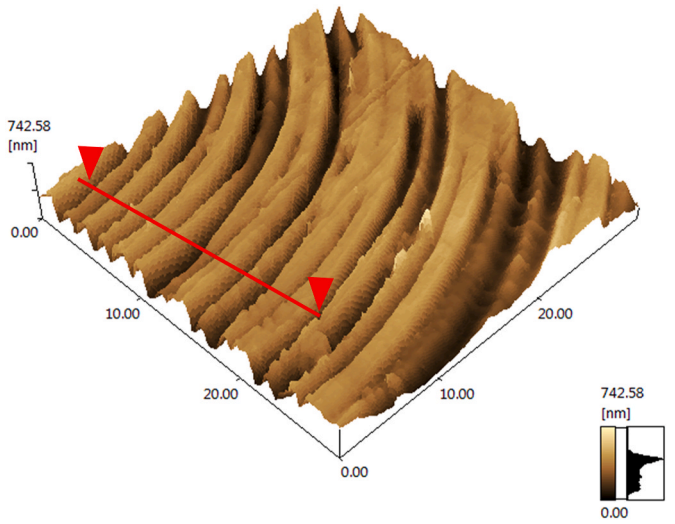

Fig. 5. The AFM image of the concentric ring structure induced by a pulse with energy of 1 mJ.

depth of the concentric ring structure is around 300 nm, and the depth of the groove does not change with the change of the radius. From this result, we might as well guess that the groove depth of the laser-induced concentric ring structure in our experiment is uniformly distributed, which can be proved by the subsequent numerical results.

In order to quantitatively study the periodic distribution of the concentric ring structure, the periodic changes of the groove along the radial direction were observed. Fig. 6 shows the height changes of the concentric ring structure along the solid line marked in Fig. 5, where the black balls show the measured results and the solid line is the result of cosine fitting. The period of the ring structure can be read directly from the fitting result, $T_m = 2$ μm. All the above experimental results show that a perfect concentric ring structure can be obtained by focusing a single femtosecond pulse at 15 μm below the surface of the fused silica. It is worth noting that the period of the concentric ring structure does not change with the radius but stabilizes at 2 μm. The micro-level periodicity and uniform distribution of the concentric ring structure make it applicable for fabricating structural color surfaces. Compared with the parallel gratings, structural color surfaces fabricated by using the concentric ring structures can eliminate anisotropy [28].

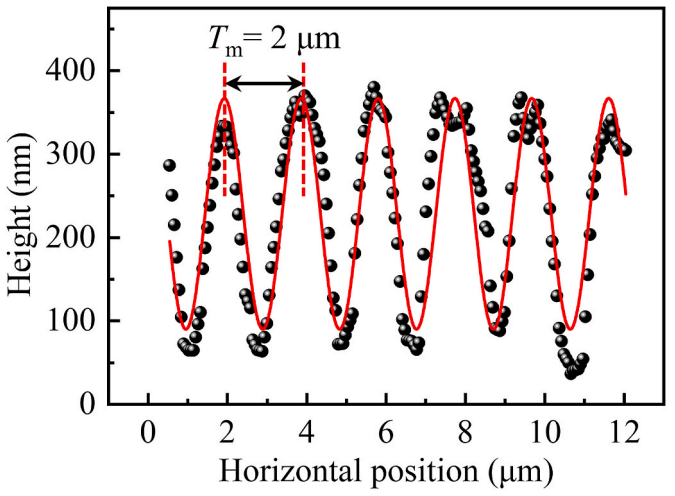

Fig. 6. The height changes of the ring structure along the solid line marked in Fig. 5, where the black balls show the measured results and the solid line is the result of cosine fitting. The period of the ring structure can be obtained, $T_m = 2$ μm.

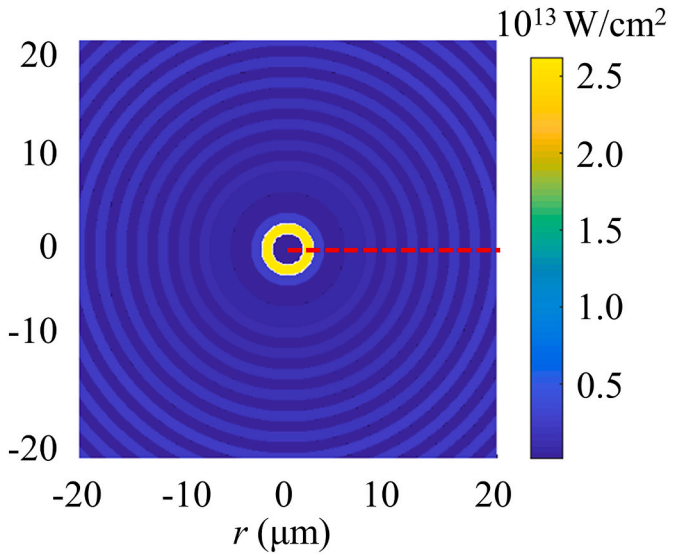

Fig. 7. The radial distribution of the light intensity at $z = 15$ μm obtained by theoretical calculation using the described model. The input pulse energy $E_{in} = 1$ mJ. The distribution of the intensity shows a ring structure.

In order to study the formation mechanism of the concentric ring structure, the radial light intensity distribution was calculated based on the nonlinear Schrödinger equation and the free electron density rate equation. Fig. 7 shows the radial distribution of the light intensity at $z = 15$ μm obtained by the theoretical calculation. The input pulse energy $E_{in} = 1$ mJ. A distinctive feature that can be seen from the radial intensity distribution is that the radial light intensity presents a concentric ring distribution, which is similar to the structure obtained by the experiment shown in Fig. 2.

In addition, the radial intensity at $r = 2$ μm is much higher than the central area and peripheral area. This special light intensity distribution can be attributed to the unique propagation mechanism of the high energy femtosecond laser pulse inside the transparent material. When the femtosecond pulse is focused inside the transparent material, self-focusing and plasma defocusing effects will dominate the subsequent propagation of the pulse. As a result, the light intensity in the central area is lower than in the surrounding areas.

The period of the concentric ring distribution of the light intensity in the calculation result is important. Fig. 8 shows the radial intensity distribution along the dotted line marked on Fig. 7. It can be seen that the light intensity presents periodic oscillations along the radial

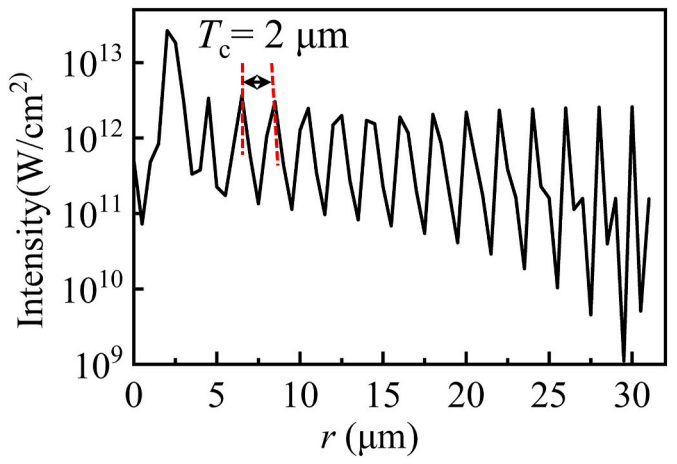

Fig. 8. The calculated result of the intensity along the radial direction. The period of the ring structure can be obtained with $T_c = 2$ μm.

direction. The period is $T_c = 2$ μm, which is consistent with the results obtained by the experiment, as shown in Fig. 6. In addition, it can be found that the peak value of the light intensity remains at about 5×10^{12} W/cm^2 along the radial direction, which suggests that the groove depth of the concentric ring structure should be kept uniform, as described in the previous paragraph. The good mapping relationship between the calculated radial light intensity distribution and the experimentally obtained structure morphology also shows that the depth of the grooves can be controlled by changing the input pulse energy.

The concentric ring structure obtained by the experimental results is in good agreement with the radial light intensity distribution obtained by the theoretical calculations. The formation mechanism of the concentric ring structure may be found from the theoretical model. The femtosecond pulse carries a large amount of energy and interacts with the fused silica. The fused silica absorbs the photon energy in the form of multiphoton absorption, forming thermal plasma, which gathers on the glass surface in an ultrashort time. The existence of plasma forms a different refractive index interface between the air and the glass. The subsequent part of the pulse is reflected when entering the plasma interface, and these reflected lights interfere with each other, resulting in a ring-shaped distribution of the light intensity. This kind of light intensity distribution led to the formation of the concentric ring structure on the glass surface.

4. Conclusion

In summary, the concentric ring structure was obtained by a single focused femtosecond pulse on the fused silica surface with pulse energy ranging from 1 mJ to 5.8 mJ. The period of these ring structures was measured to be 2 μm. The dependence of the diameter of the ablation area on the input pulse energy has been demonstrated, showing a linear relationship. In addition, a model based on the nonlinear Schrödinger equation and the free electron density rate equation has been used to calculate the light intensity distribution along the radial direction. The theoretical results are in good agreement with the experimental results. The consistency between the theoretical and experimental results allows us to read the distribution of light intensity from the structural features. The results can be expected to provide a new perspective for the exploration of the mechanism of laser-induced concentric ring structure formation. Furthermore, the concentric ring structures have a good prospect for the fabrication of isotropic structural color surfaces.

Declaration of competing interest

The authors declare that they have no known competing financial interests or personal relationships that could have appeared to influence the work reported in this paper.

Acknowledgment

This work was funded by the National Natural Science Foundation of China (Grant No. 51975232, 51727809). The authors would like to express their thanks for the technical support from the Experiment Center for Advanced Manufacturing and Technology in the School of Mechanical Science & Engineering of HUST. The authors appreciate the kind proofreading support provided by Ms Lucille Serody and Mr. Robert Serody.

References

[1] Gattass RR, Mazur E. Femtosecond laser micromachining in transparent materials. Nat Photonics 2008;2:219–25.
[2] Bonse J, Kirner SV, Krüger J. Laser-induced periodic surface structures (LIPSS). In: Sugioka K, editor. Handbook of laser micro-and nano-engineering. Switzerland: Springer International Publishing; 2020. p. 1–59.
[3] Bonse J. Quo vadis LIPSS?—recent and future trends on laser-induced periodic surface structures. Nanomaterials 2020;10:1950.
[4] Bonse J, Gräf S. Maxwell meets marangoni—a review of theories on laser-induced periodic surface structures. Laser Photon Rev 2020;14:2000215.
[5] Gräf S. Formation of laser-induced periodic surface structures on different materials: fundamentals, properties and applications. Adv Opt Technol 2020;9:11–39.
[6] Zheng HY, Zhou W, Qian HX, Tan TT, Lim GC. Polarisation-independence of femtosecond laser machining of fused silica. Appl Surf Sci 2004;236:114–9.
[7] Chambonneau M, Grua P, Rullier JL, Natoli JY, Lamaignère L. Parametric study of the damage ring pattern in fused silica induced by multiple longitudinal modes laser pulses. J Appl Phys 2015;117:103101.
[8] Shi X, Jiang L, Li X, Zhang K, Yu D, Yu Y, Lu Y. Temporal femtosecond pulse shaping dependence of laser-induced periodic surface structures in fused silica. J Appl Phys 2014;116:033104.
[9] Gräf S, Kunz C, Müller FA. Fabrication of versatile functional surface properties based on femtosecond laser-induced periodic surface structures (LIPSS). In: International society for optics and photonics, proc SPIE, vol. 11268; 2020, 112680S.
[10] Shi X, Xu X. Laser fluence dependence of ripple formation on fused silica by femtosecond laser irradiation. Appl Phys A 2019;125:1–8.
[11] Vorobyev AY, Guo C. Direct femtosecond laser surface nano/microstructuring and its applications. Laser Photon Rev 2013;7:385–407.
[12] Fang Z, Shao J. Femtosecond laser-induced periodic surface structure on fused silica surface. Optik 2016;127:1171–5.
[13] Schwarz S, Rung S, Esen C, Hellmann R. Surface plasmon polariton triggered generation of 1D-low spatial frequency LIPSS on fused silica. Appl Sci 2018;8:1624.
[14] Shen C, Zhao N, Pribošek J, Ma M, Fang L, Huang X, Zhang Y. Characteristics of optical emission during laser-induced damage events of fused silica. Chin Opt Lett 2019;17:123002.
[15] Heins A, Guo C. Shock-induced concentric rings in femtosecond laser ablation of glass. J Appl Phys 2013;113:223056.
[16] Heins AM, Guo C. Spatial mode cleaning in radically asymmetric strongly focused laser beams. Appl Phys B 2013;B113:317–25.
[17] Liu Y, Brelet Y, He Z, Yu L, Forestier B, Deng Y, Jiang H, Houard A. Laser-induced periodic annular surface structures on fused silica surface. Appl Phys Lett 2013;102:251103.
[18] Zhang X, Jiang Y, Qiu R, Meng J, Cao J, Zhang C, Zhao Y, Lü T. Concentric ring damage on the front surface of fused silica induced by a nanosecond laser. Opt Mater Express 2019;9:4811.
[19] Tzortzakis S, Sudrie L, Franco M, Prade B, Mysyrowicz A, Couairon A, Bergé L. Self-guided propagation of ultrashort IR laser pulses in fused silica. Phys Rev Lett 2001;87:213902.
[20] Sudrie L, Couairon A, Franco M, Lamouroux B, Prade B, Tzortzakis S, Mysyrowicz A. Femtosecond laser-induced damage and filamentary propagation in fused silica. Phys Rev Lett 2002;89:186601.
[21] Gulley JR, Winkler SW, Dennis WM, Liebig CM, Stoian R. Interaction of ultrashort-laser pulses with induced undercritical plasmas in fused silica. Phys Rev A 2012;85:013808.
[22] Gulley JR, Winkler SW, Dennis WM. Simulation and analysis of ultrafast-laser-pulse induced plasma generation in fused silica. Opt Eng 2008;47:054302.
[23] Song J, Wang X, Hu X, Dai Y, Qiu J, Cheng Y, Xu Z. Formation mechanism of self-organized voids in dielectrics induced by tightly focused femtosecond laser pulses. Appl Phys Lett 2008;92:092904.
[24] Zhang L, Liu J, Zhong Z, Jiang H, Gu H, Chen X, Liu S. Beam collapse and refractive index changes inside fused silica induced by loosely focused femtosecond laser. J Opt 2021;21:075402.
[25] Sun W, Qi H, Fang Z, Yu Z, Liu Y, Yi K, Shao J. Nanosecond laser pulse induced concentric surface structures on SiO_2 layer. Opt Express 2014;22:2948–54.
[26] Cao H, Shu X. the formation of concentric rings induced by defocusing femtosecond laser on Si surface. In: Asia communications and photonics conference. Optical Society of America; 2016. AS1J-3.
[27] Zhang L, Liu J, Gong W, Jiang H, Liu S. Diffraction based single pulse measurement of air ionization dynamics induced by femtosecond laser. Opt Express 2021;29:18601–10.
[28] Liu W, Hu J, Jiang L, Huang J, Lu J, Yin J, Qiu H, Liu H, Li H, Wang S, Wang S. Formation of laser-induced periodic surface nanometric concentric ring structures on silicon surfaces through single-spot irradiation with orthogonally polarized femtosecond laser double-pulse sequences. Nanophotonics 2021;10:1273–83.